Spectrum of Engineering Sciences
ISSN (e) 3007-3138 (p) 3007-312X Volume 4, Issue 6, 2026

# OXYGEN EVOLUTION REACTION BY USING PHOTOANODIC $TA_3N_5$ FOR WATER SPLITTING PROCESS BY DIFFERENT SURFACE MODIFICATION: A REVIEW

**Toaqeer Salman[1], Sumera Zaib[*2], Hafiz Saqib Ali[3], Aisha Nawaz[4]**

[1,*2,4]*Department of Basic and Applied Chemistry, Faculty of Science and Technology, University of Central Punjab, Lahore 54590, Pakistan*
[3]*Department of Pure and Applied Chemistry, University of Strathclyde, 295 Cathedral Street, Glasgow, G63 9BP, United Kingdom*

[*2]sumera.zaib@ucp.edu.pk

DOI: https://doi.org/10.5281/zenodo.20588510

**Keywords**
*Fossil, renewable energy, semiconductor, band structure, nanocomposite, water splitting.*

**Article History**
*Received: 09 April 2026*
*Accepted: 21 May 2026*
*Published: 08 June 2026*


**Corresponding Author: ***
**Sumera Zaib**

**Abstract**
*Fossil energy is a widely used energy source these days, but because of the fossil usage; many complications also arise. In response, a global shift toward sustainable and renewable energy sources has amplified interest in photoelectrochemical (PEC) water splitting as a viable route for clean hydrogen production. Water splitting, which involves the decomposition of water into hydrogen and oxygen, depends critically on the development of efficient and stable semiconductor photoanodes. For this reason, many semiconductors are used; but titanium nitride ($Ta_3N_5$) semiconductor has great importance because of the low-over potential, better band structure, lesser charge transfer resistance (Rct), decreased solution resistance (Rs), maximum current density and abundance. However, the practical application of $Ta_3N_5$ is limited by poor charge mobility, surface instability, and rapid electron-hole recombination. To overcome these limitations, significant research has been carried out to prepare the nanocomposites of $Ta_3N_5$ such as nanofibers, nanofilms, micro sheets, dum bell-like nanostructures, and nanoflowers. These varied morphologies not only enhance visible-light harvesting and charge separation but also lower overpotential and suppress recombination losses, thus improving the overall efficiency of PEC water splitting. Furthermore, a variety of synthetic methodologies including hydrothermal, sol-gel, electrospinning, electrochemical, precipitation, and chemical reduction techniques helped in achieving uniform doping, nanoscale control, and enhanced structural stability. In conclusion, $Ta_3N_5$ is of significant interest in semiconductor research for water splitting applications. However, future research must focus on improving long-term operational stability, enhancing charge transport across interfaces, and integrating $Ta_3N_5$ into tandem PEC cells or hybrid solar fuel systems.*

## 1. INTRODUCTION

Environment is polluted as fossil fuels are used widely as a major energy source that leads to the global warming and other complications. Another alarming complication is the limited fossil fuels that are being used on daily basis to meet the energy requirements [1]. Solar energy is abundant source of energy. Semiconductor

photoelectrochemical cells (PEC) is widely used to convert solar energy into chemical energy which is called as STH to reduce world energy problems. Fossil energy is the biggest energy source these days, but as World is shifting to renewable energy source as solar and specifically fuels which is Hydrogen by PEC to get water splitting shows a renewable energy [2]. To convert solar energy into chemical energy, water splitting through solar is a better mean to sort out the power crises.

It is common fact regarding the usage of fossil energy in the region could also lead to the various issues, as it brings pollutants to the environment like the Sulphur dioxide, and Nitrogen dioxide which are the basic cause of the acid rain, and everyone is familiar with the negative impacts of the acid rain in the environment [3]. Many complications have come to the surface like different cyclones in different countries of the world, melting of the glaciers due to the greenhouse effect that have caused severe flood in different regions of India and Pakistan back in the year of 2022. Therefore, World is shifting from the non-renewable energy source to the renewable energy source to fulfil the energy requirements of the World. For the energy production by eco-friendly environment is made possible because of many ways like the wind energy, hydropower, geothermal and solar energy sources etc are the main energy sources in this world.

### 1.2 Effects of Fossil consumption

Existence of the humankind on this planet is only way possible if the clear source of energy is available, then it is a way possible for the stable life [4]. There are many ways to get the energy, for many years, only reliable was the fossil energy. Fossil energy is carbon-based materials [5]. These fossil fuels are the main cause of the environmental hazards, as rising level of $CO_2$, heat and other pollutions [6]. It is the major source of the global warming, as the $CO_2$ increases, it brings the temperature to 0.5 $^0$C rise every 2 to 3 years [7]. Fossil fuels burning in the automobiles, causes the emission source of the acid rain. So the major shift is required from non-renewable energy source to the renewable energy source as reported in the study given by [8]. It is stated that the global energy supply was 16.7 TW in 2007 according to the energy data [9]. This energy demand has increased, as the World population is increasing day by day [10]. As the World population would reach 9.5 billion in 2050, as this addition in population would also increase the demand of the energy [11]. Energy supply would not be fulfilled by carbon-based fossil fuels, there alternative ways to produce and utilize energy is very important. The energy supply of the World would be 30 TW in 2050. This increase from 16 TW to 30 TW, requires more sources of energy [12]. This low energy supply by the biomass consumption, secondly nuclear energy requires more sites that are difficult to build by that year. If the only reliable source would be fossil fuels, then the level of atmospheric $CO_2$ would also be doubled [13].

### 1.3 Renewable Energy shift

Therefore, the better and reliable source is sun, as the sunlight is the only renewable energy source that can meet the energy crises of the World [14]. The major challenge is the harvesting of the sunlight radiations, like to convert she solar energy into the chemical energy. Therefore, the solar panels are widely used cells to harvest the solar energy [15].

Water splitting process was basically introduced to World by Fujishima and Honda in 1972 which led to the new ways of producing energy. Fossil fuels were majorly used to meet the energy problems of the World, and in the same year, Fujishima and Honda performed the Hydrogen evolution with the help of the semiconductor titanium oxide [16]. Since then, huge work has been done on the photoanodes for the effective semiconductors to absorb the maximum visible light better electrical and conduction.

Solar energy is the abundant source of energy on the planet Earth, and semiconductor photoelectrochemical cells (PEC) are widely used to convert the solar energy to the chemical energy i.e. Hydrogen by water splitting [17]. Main anodes that are being used for the water splitting have great importance regarding the effectiveness and firmness [15]. It is reported that sunlight which reaches the earth's surface is $8.6 \times 10^4$ TW which is much more than the annual consumption of

energy by human being that is close to 19 TW [18]. Sunlight comprised half of the visible light spectrum whose wavelength range exists from 300-800 nm. It is the major portion of the sunlight so to use the wavelength of this range is quite accomplishable [16].

**1.4 Hydrogen as the Important Energy source**

Hydrogen can be consumed as the catalyst in the chemical and petroleum industry as a reducing agent. It is reported in study that hydrogen is produced 50 megatons in the world every year, but all this is produced by non-renewable and renewable energy sources [19]. The world is trying to meet the energy requirements, so hydrogen can also be obtained by the other renewable methods like the water splitting by thermochemical, electrochemical, PEC water splitting, and right now, only electrolysis of water is present at the commercial level [20]. But, hydrogen production by using renewable electrolysis water splitting is very low as only 4% can be obtained by this method [21].

Therefore, the requirements of searching for sustainable alternative energy sources for the creation and the storage of energy have increased [22]. Water splitting is basically a process in which water is used to produce the hydrogen ($H_2$) and oxygen ($O_2$) gasses as this is the most economical and environmentally friendly method [23]. The process of electrolysis involves passing an electric current through water, which releases hydrogen ($H_2$) and oxygen ($O_2$), as water is widely available [22]. As it goes, a schematic depiction of the image is given below in the Figure 1.1, which shows how the conduction band and valance band shows the water splitting with the help of light.

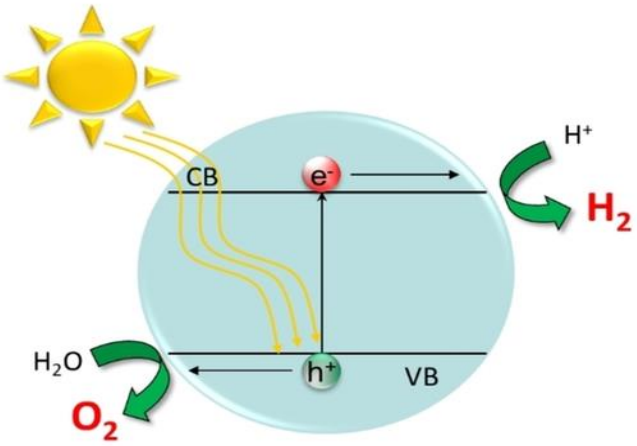


**Figure 1. Schematic representation of the photocatalysis for the hydrogen or oxygen generation [24] Produced Under common creative license 3.0.**

**1.2 Basic Principle of Electrochemical water splitting**

As far as water splitting is concerned, two phenomena are essential to understand; one is oxygen evolution reaction called as OER that occurs at anode; because of the anodic potential and Hydrogen evolution reaction that also called as HER occurs at cathode; because of the cathodic potential [25]. In both of these OER is comparatively a slow process because of the 4 e-lectrons to transfer while forming reaction intermediates [26]. Ruthenium oxide or iridium oxide is used for OER and platinum is used for the HER in the basic as well as acidic medium [27].

$H_2O \rightarrow H_{2\,(g)} + 12\ O_{2\,(g)} \rightarrow$ (1)

And for water splitting, two reactions are very important to understand as one reaction depicts the reaction of HER and OER as given below in the equations (2) and (3) respectively:

HER: $2H^+_{(aq)} + 2e^- \rightarrow H_{2\,(g)}\ E^0 = 0.00\ V \rightarrow$ (2)

OER: $2H_2O \rightarrow O_{2\,(g)} + 4H^+_{(aq)} + 4e^-$ $E^0 = 1.23$ V → (3)

As HER reaction takes place at the cathode, and the OER reaction takes place at the anode as given in the above equations (2) and (3), respectively.

### 1.2.1 Mechanism of OER

The OER occurs in three different medias as alkaline, neutral as well acidic media [28]. The pH is highly involved this reaction as four electron-proton coupled reactions are involved in this reaction [29]. Four protons are obtained from two $H_2O$ molecules are oxidized, and besides this Oxygen molecule is also obtained in two different medias like acidic as well as neutral media [30]. Further explanation about this reaction is understanded with the following reactions [31];

$4OH^- \leftrightarrow 2H_2O\,(l) + O_2\,(g) + 4e^-$ Alkalic solution (1)

$2H_2O\,(l) \leftrightarrow 4H^+ + O_2\,(g) + 4e^-$ Acidic solution (2)

With the help of electrochemistry of OER as their potentials can be seen according to reaction mixture.

$2H_2O \rightarrow O_2 \uparrow + 4H+ + 4e\text{-}$ E=1.229V

Above given potential of photoanodic reaction is in an acidic solution electrolytic reaction, while below given photoanodic potential is given for the alkaline electrolytic reaction:

$4OH\text{-} \rightarrow O2 \uparrow 2H2O + 4e\text{-}$ E=0.401V

As far as the protic reactions are concerned, that are explained in the above given reactions, but for the aprotic reactions in which no Hydrogen and Oxygen bond is present in any solvent:

$O2\text{–}2 \rightarrow O2 \uparrow + 2e\text{-}$[32]

### 1.2.1 Oxygen evolution reaction by $Ta_3N_5$

The photoanodes are made up of the semiconductors [33]. As far as the properties of the photoanodes are concerned, it could absorb the maximum visible light from the sunlight, better ability to transfer the electrons to the other electrode [34]. Many techniques have been used to modify the photoanodic efficiency of the semiconductor; and doping with element, heterojunction and surface modification [35]. Semiconductors which match with these properties are include bismuth sulphide, bismuth vanadate, tungsten oxide, molybdenum oxide iron oxide, tantalum nitride and titanium oxide; specifically, the property of high electron transfer and better absorption of light [36]. From all the techniques to increase the efficiency of photoanodes, heterojunction is very important for the better absorption of the light. This technique is being used to enhance the photoelectrochemical performance, as this heterojunction could efficiently separate the electron-hole ($e^-/h^+$), and maximum ultra-violet visible light absorption [37]. Despite this heterojunction, another important technique which can enhance the photoanodic response for the oxygen evolution response as with the help of co-catalyst [38].

The light falls out on the surface than degradation of the surface will occur and to overcome that specific problem, further surface modification of the OER catalysts suggested [39]. Many tandem PEC cells have been developed for better efficiency to produce 10% of Hydrogen, but most difficult thing in tandem PEC cells is designing of the stable photoanode OER for the evolution of oxygen under sunlight irradiation [40]. For this purpose, Tantalum nitride is a better photoanode for oxygen evolution during the water splitting method. But its stability is difficult to attain and photoconversion efficiency is low due to poor electrical mobility [41].

Light absorption is directly associated with the intrinsic properties like the carrier diffusion, electron and carrier transport of semiconductor $Ta_3N_5$ [42]. Semiconductor's electrolyte solution interface, catalytic activity and the mass transfer of electrons should also be ascertain to check water splitting efficiency [43]. Many electrolytes and the metal oxides have been used to dope the surface of semiconductor Tantalum Nitride to improve the PEC cells efficiency for more oxygen evolution from the cell. By using new more probes can be used to grow the water splitting efficiency of the cells as discussed in this paper [44].

## 2. Surface modifications

The PEC cells consist of two electrodes as photoanode and photocathode. The efficiency of

these cells can be increased. This review totally emphasizes the total emphasize on the surface modification of the Tantalum Nitride semiconductor. Many electrocatalysts likewise Nickel, Iron and Cobalt species were doped on the surface of $Ta_3N_5$ semiconductor to see the effects of PEC cells and its efficiency [45].

### 2.1 $SiO_2$ Doping

Tantalum nitride ($Ta_3N_5$) has received importance due to the minimum energy level of CB and maximum energy level of VB, which lead to absorption of visible light that's why efforts have made to construct the semiconductors which are responsive to visible light [46].

$Ta_3N_5$ doped with the Aluminium and the Tantalum doping, both are the photocathode which are special in absorptive wavelength of 780 nm for water splitting [47]. In order to make tandem PEC cells, both sides of transparent $Ta_3N_5$ doped with the $SiO_2$ as discussed earlier that tandem semiconductor efficiency is much better than the parallel PEC cell so that's why transparent $Ta_3N_5$ is made tandem. Therefore, current study leads to the main point that the tandem PEC cells now have two sides as one side acts as photoanode and the back side acts as photocathode while using semiconductor $Ta_3N_5$ doped with $SiO_2$ [48].

### 2.2 Metal Oxide Doping

Its stability and photoconversion can be enhanced with the help of surface modification as nanostructure designing and doping of semiconductor with the other metal, because by doing this thickness of semiconductor has also impact on the PEC cells [49]. But with the thicker photoelectrode, problem usually happens of poorer charge-transfer ability due to factor of light scattering and reflection. In this study, it was noticed that nano films of PEC cells have much better efficiency as water splitting is on the 240 nm while thicker PEC cells showed very lower performance at 750nm as increased charge recombination rate [50].

In this study, problems of PEC cells were improved, as various cells with various thickness were prepared as by oxidation and nitridation of the Ta foils. As far as semiconductor photoanodes are concerned, two different thickened photoanodes $Ta_2O_5$ and $Ta_3N_5$, Tantalum nitride show less attachment to the substances, so to sort out this problem, porous structure has been developed as lesser light will reflect out and scattering will also be decreased and porous surface will allow more co-catalyst addition to the surface [51].

Ta3N5 Tantalum nitride ($Ta_3N_5$) has been widely used because of the small energy gap which is 2.1 eV as well as stability. Other significant property of this semiconductor is that it does not need any sort of assist for solar water splitting as other electrodes required assist to do water splitting and its splitting of water is spontaneous as a single photoanode [52]. Tantalum nitride oxides photocurrent potential curves are shown in the below given diagram for Nickel Iron cobalt oxides, Nickel Iron oxides, Cobalt oxides, Nickel oxides, and Iron oxides which are for the oxygen evolution reaction, as simulated sunlight $Ta_3N_5$ photoanodes generated anodic current. While using all these oxides, current production can be increased as increase the photoelectrode potential [53]. NiFeCoOx, NiFeOx oxides surface modification has set up the photocurrent potential to 0.7 comparatively vs RHE. If these oxides are compared with the $NiO_x$ / $Ta_3N_5$ / Ta photoanode has increased linearly, while hole transfer efficiency for NiOx is weak as compared to the mixed metal oxides as mentioned above [52]. As far as the oxides of FeOx are concerned, its photoanode show low photocurrent as compared to the $Ta_3N_5$ / Ta to get the oxygen evolution reaction, as light absorption in the FeOx is very insignificant, because it shows Iron oxide's light halting does not cause the low PEC cell's performance.

The performance of different photoanodes like NiFeCoOx/ $Ta_3N_5$ /Ta, CoOx/ $Ta_3N_5$ /Ta and NiFeOx$Ta_3N_5$ /Ta measured at the 0.7 vs. RHE under the simulated light, and it is reported Nickel Iron oxide was able to generate the 0.36 $mAcm^{-2}$ photoanodic current density after 1 minute, which decreased after 5 minutes. NiFeOx/ $Ta_3N_5$ /Ta could also generate the photoanodic current density of 0.40 $mAm^{-2}$ after 1 minute, and that was

retained up to 0.36mAm$^{-2}$ after 5 minutes. It is much lower current density comparatively to other photoanodes of 0.03 mAcm$^{-2}$ was generated by the CoOx/ $Ta_3N_5$ /Ta. The photocurrent density can be increased by surface modification of the $Ta_3N_5$ through Co(OH)x co-catalyst that is 2.8 mA/cm$^{2.}$ [53]. Co (OH)x was coated on Tantalum nitride by impregnation method.

## 2. Nano-structuring of $Ta_3N_5$

$Ta_3N_5$ has poor charge transport and lesser CoPi/ $Ta_3N_5$ /Ta light energy positions to get the absorption bands of long wavelength light, efficient charge separation bulk and surface defects absorption [54]. Therefore, to overcome this suffering as morphology control with a 1D configuration, such as nanotubes (NTs), nanorods' (NRs) and all these strategies advances the charge transfer to the solid-liquid interface with high absorption of light [55]. For this this reason, different nano structuring and morphology is being discussed here.

### 2.1 $Ta_3N_5$ Films

The expected results of photocatalytic activity can be obtained by the interface between electrolyte and semiconductor to produce the charges, and the second important tool that is to accelerate this charge across the interface [56]. Basically, co-catalysts are deposited on the $Ta_3N_5$ for the charge transferring between the electrolyte and semiconductor. The important co-catalysts that are used to produce the photogenerated holes in the $Ta_3N_5$ and also avoid the electrons to recombine with the catalysts surface for the efficient oxygen evolution reaction [57]. This includes Iron (III) oxide hydroxide, Nickle Iron layered double layer, cobalt hydroxide, and cobalt-principle investigator (CoPi) to generate and avoiding holes to recombine with the $Ta_3N_5$ [58]. It is reported in a study that the more active co-catalyst which can improve the efficiency of the interface charge transformation Co-Pi/GaN bilayer. This heterojunction combination of the $Ta_3N_5$ and cobalt hydroxide can lead to the maximum solar water splitting [59]. For maximum solar water splitting, cobalt based co catalysts are considered as the most efficient co-catalysts. The one condition which makes it the efficient co-catalyst is the basic ratio of $Co^{2+}/Co^{3+}$ in the cobalt oxide [60]. Furthermore, the plasma treatment also increases the solar water splitting by creating the maximum vacancies [61].

$Ta_3N_5$ is basically an n-type photoanode for water splitting, with the band gap of 2.1 eV which ultimately lead to the maximum current density [62]. The main motive behind the synthesis of the tantalum films is the excessive energy usage, because the substrates are need to expose the ammonia at the 600 $^0$C with the very weak adhesion. Therefore, due to this weak adhesion, the conductivity of the substrates $Ta_3N_5$ become very low [63]. This problem is sorted out by the atomic layer deposition (ALD) by preparing the tantalum doped films and deposing these films on the TTO ($TiO_2$). The synthesized films are amorphous at first, but this surface is further improved by the nitridation of the amorphous films of the tantalum nitride [64].

$Ta_3N_5$/GaN/$Al_2O_3$ are the crystal clear designated 600 nano meter absorption limit of the $Ta_3N_5$. Ta-$_3N_5$ films were prepared substrate by radiofrequency (RF) with the help of sputtering and this spiting focus was a Tantalum disk with a 50 nm diameter and a thickness of 3mm and Argon atmosphere for no less than ten mins for cleaning purpose [65]. By using quartz including quartz $SiO_2$ and bare sapphire Al2O3, thin films transparent $Ta_3N_5$ were prepared resulting high transparency above 600 nm [64].

### 2.1 $Ta_3N_5$ Nanoflowers

$Ta_3N_5$ nanoflowers can be prepared through a simple hydrothermal method [66]. The nanosized structures preparation of the photocatalyst is only way possible to increase the photocatalytic activity by the heterojunction [67]. Therefore, this nanoflower structure is made by combining the semiconductors like Iridium oxide, cobalt oxide, tantalum oxide nitrate and silver nitrate with the $Ta_3N_5$ by the heterojunction method [68]. Basically, the deposition of the metals like silver, gold and platinum on the $Ta_3N_5$ increases the photocatalytic activity [69]. The nonwoven clothes of the $Ta_3N_5$ are prepared in one study with the help of $Ta_3N_5$-Pt heterojunction, because this is the effective tool to increase the photocatalytic

activity [70]. A possible mechanism for the synthesis of $Ta_3N_5$ nanoflowers are done with the heterojunction of $Ta_3N_5$-Au coupling to improve the photocatalytic activity [71].

As far as the main reactants are concerned for the synthesis, tantalum oxide, tantalum chloride are added into the Teflon heated at the temperature of 850 $^0$C with the solvothermal method. The temperature range is very important for the synthesis of flower-like nanostructures of the $Ta_3N_5$ [72]. The heterojunction flower-like structure of the $Ta_3N_5$-Au is via the Facile wet impregnation method by using the microspheres of the main catalyst [73]. Furthermore, the flower-like preparation of the electrocatalyst is demonstrated in the below given Figure 2.1.

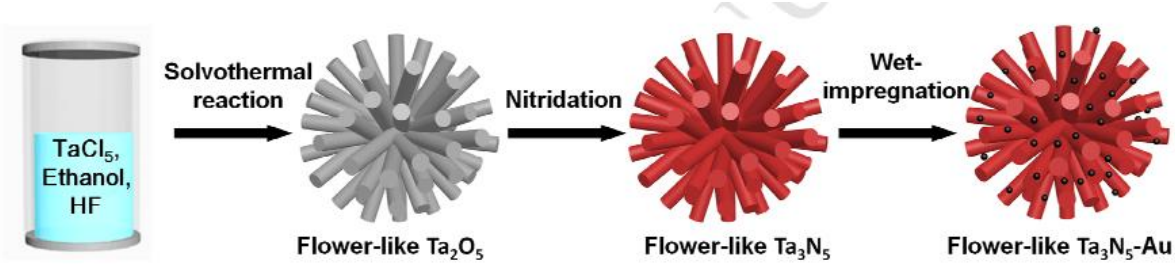


**Figure 2. Schematic preparation of the Flower-like nanostructure of $Ta_3N_5$-Au [71] Produced Under common creative license 3.0.**

This type of nanostructures includes $Ta_3N_5$-Au, $Ta_3N_5$-Pt, $Ta_3N_5$-Ag, $SiO_2$-Au and bulk $Ta_3N_5$. In the given study, photocatalytic activity of these nanosized structures is calculated by the degradation of the MB i.e., methylene blue after reaction of 60 minutes [74].

| Catalyst | Degrading %age of MB |
|---|---|
| Bulk $Ta_3N_5$ | 60.3 |
| Flower-like $Ta_3N_5$ | 76.1 |
| Bulk $Ta_3N_5$-Au | 81.7 |
| Flower-like $Ta_3N_5$-Au | 100 |

Consequently, different nanosized structures of the $Ta_3N_5$ are compared to improve the photocatalytic activity. Flower-like nanostructures showed better photocatalytic activity than the bulk $Ta_3N_5$. The flower-like structure of Flower-like $Ta_3N_5$-Au exhibited high degradation of the methylene blue (MB) in the time of 60 minutes reaction.

### 2.3 Olive-like structures $Ta_3N_5$

It is reported that Olive-like structure of $Ta_3N_5$ is prepared with the help of hydrothermal method in which Tantalum chloride and sodium amide [75]. The main reactants, as both these are heated at 200 °C for 12 hours, then calcination at 600 °C for 2 hours to obtain the final product [76]. The explanation of the hydrothermal method is given in the following paragraph. The controlled nanostructure like olive-like structure of $Ta_3N_5$ and high purity simple oxides and nano sized spinel can be prepared with this hydrothermal method as its morphology can be adjusted the reaction's temperature and pressure [76]. For the preparation of this method, With the help of continuous stirring of aqueous solution KOH or NaOH are mixed with the metal salts which includes acetate, chloride and nitrate, then this mixture is autoclaved in which the solvent is sealed and heated for several hours to obtain the products [77].

The photocatalytic activity of the olive-like porous structure of $Ta_3N_5$ is assessed on the base of the catalytic degradation of the methylene blue (MB), just like the flower-like structure showed the activity on the degradation process [78]. Therefore, the hydrothermally synthesized materials

exhibited the higher degradation of the $Ta_3N_5$ under the visible light [79]. Another study was conducted on the degradation of the phenol by the porous material of $Ta_3N_5$, as confirmed by the different morphological techniques [80]. It is reported in the study that the porous materials i.e., olive like structure of the exhibited higher degradation of the methylene blue (MB) and phenol as compared to the rod-like structure of the nanocomposites of $Ta_3N_5$ [81].

### 2.4 Micro-sheets of $Ta_3N_5$

Other composites are the micro sheets of $Ta_3N_5$ that can be prepared by various ways, but most promising methods are hydrothermal, template assisted synthesis and solvothermal method [82]. As far as the template assisted synthesis is concerned, it is being prepared with the help of ammonium metavanadate as a template, as these sheets gave the thickness of 100 nm, a length of several micro sheets [83]. The purpose of using this template so that the length of the nanocrystals of the $Ta_3N_5$ crystals can be controlled [84]. Mesoporous silica nanoparticles (MSN) are used as the template in the method of chemical reduction method for the preparation of the $Ta_3N_5$ in the form of micro sheets [85].

This the method to make metal nanoparticles, a reducing agent is dissolved in water, often sodium borohydride [86]. Reducing agents are sometimes mixed with stabilizing agents [87]. Absorbance analysis examined the dispersion stability of metal nanoparticles. There are a number of drawbacks that are connected with reducing agents, including their toxicity, increased price, limited capacity to reduce, high costs, and impurities [88].

### 2.5 Dumbbell-like Nanostructures of $Ta_3N_5$

Dumbbell-like nanostructures of $Ta_3N_5$ have been synthesized using various methods. One such method is the hydrothermal synthesis route [89]. In their study, $TaCl_5$ and urea were used as precursors, and the reaction was carried out in a Teflon-lined stain less steel autoclave at 200 °C for 24 h [90]. The dumbbell-like nanostructure of $Ta_3N_5$ is usually range of a diameter of 80-120 nm [89]. The synthesis of dumbbell-like $Ta_3N_5$ nanostructures is also possible by using a solvothermal method and microwave-assisted hydrothermal method [78]. In these methods, the resulting product was a dumbbell-like nanostructure of $Ta_3N_5$ with a diameter range of 100-200 nm [78].

In summary, dumbbell-like nanostructures of $Ta_3N_5$ have been synthesized using various methods such as hydrothermal, solvothermal, and microwave-assisted hydrothermal methods [52]. The bests among all methods, is hydrothermal method, because the nanocomposites is of the very narrow range and are considered good nanocomposites for the applications [91].

### 2.6 $Ta_3N_5$ Nanotubes

According to the recent studies, plasma-inscribed Cobalt oxide showed a high ratio of $Co^{2+}/Co^{3+}$ with the help of higher current density and lower potential that was performed on the Ar-inscribed Cobalt oxide NSs with oxygen vacancies assigned to high $Co^{2+}$ population with the active sites for Oxygen evolution reaction [92]. The interactive impression of depletion of recombination centre on the interface and high oxygen voids of Cobalt hydroxide showed in higher activity of the photoanodes for the $Ta_3N_5$ [93]. The Co (OH)x/Tantalum Nitride for the atomic ratio of $Co^{2+}/Co^{3+}$ directs to the more $Co^{2+}$ concentration can lead to the surface oxygen vacancies induced in the Ar plasma [94]. The Cobalt hydroxide electrode directs to the much better water splitting activity on Ar-plasma-treated Co (OH)x for OER [92]. Another important function of the Ar-plasma on the surface of nanotubes of $Ta_3N_5$ caused the less defect densities, and the comparative density of $Co^{2+}$ and $Co^{3+}$ is related to the oxygen voids [94].

### 2.7 $Ta_3N_5$ Nanoparticles

Solutions with low energy with nanoparticles are considered to be the better incorporator of the light [95]. Photocatalysts are used as a renewable energy materials [17]. Many materials are important like quantum dots, carbon-based and metal oxide nanoparticle materials [96]. It is reported in different studies about the nanoparticles of Tantalum nitride, as it demonstrated higher photocatalytic activity [97]. Different methods are undertaken for the

preparation of $Ta_3N_5$ nanoparticles, but the best of one is the diffusion of nitrogen on the surface of Tantalum oxide [98]. It is the potential candidate with the band gap of 2.08 eV [99].

The photocatalytic activity of the $Ta_3N_5$ nanoparticles is reported with the different agents [100]. The activity of the material is reported by the degradation of the organic pollutants [101]. The higher degradation reported is of the methylene blue with the nanoparticles of the $Ta_3N_5$ [102]. The nanoparticles are synthesised with the help of the carbon nitride $C_3N_4$ , which can act as template and nitrogen source [103].

In conclusion, $Ta_3N_5$ nanoparticles demonstrated the highest durability than any other nano structure of these material. It is considered to be the better material version for the OER and its stability.

## 3. Electrochemical measurements Parameters

The following important parameters are used to assess the electrochemical performance of the electrocatalyst. All the details are given in the following data;

### 3.1 Over Potential for OER

The electrochemical activity, there's the phenomenon which is of great importance is the over potential. To reduce over potential, electro catalysts are being used for OER to lower the over-potential and increase the charge separation capacity [105]. NiFeOx is being used to generate the holes under light and the other important reason to use this electrocatalyst is that it lowers the over potential [106]. It is reported that the over potential of the single metals is high as compared to the other composites which are adhered to it [107]. Single metal in blue which is the hybrid nanocomposite is the great in terms of the over potential, while the multi-metal oxides are also in the good position for lowering the over-potential [108]. This study is to highlight the potential of $Ta_3N_5$ as an efficient catalyst for the OER and provide valuable insights into its electrochemical performance in terms of overpotential [106].

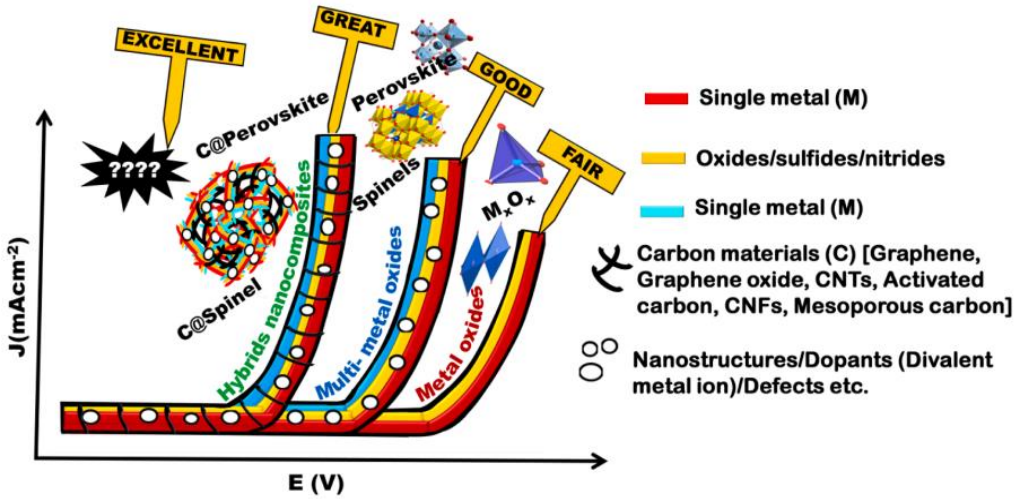


**Figure 3. Schematic diagram shows the over potential of the metal nitrides, decreased after by surface modification with other composites [108]. Produced Under common creative license 3.0.**

### 3.2 Tafel Slope for OER and Double-layer Capacitance

The Tafel slope plays a crucial role in understanding the oxygen evolution reaction (OER) kinetics. It provides valuable insights into the reaction mechanism and the electrochemical behaviour of catalysts involved in water splitting processes. The Tafel slope is defined as the slope of the linear relationship between the logarithm of the OER current density and the applied overpotential. The Tafel slope for the oxygen

evolution reaction (OER) by $Ta_3N_5$ has been reported to be approximately 40-60 mV/dec [109]. Double layer capacitance refers to the charge storage capacity at the interface between an electrode and an electrolyte solution. [110] examined the electrochemical properties of $Ta_3N_5$ and demonstrated its high double layer capacitance and charge storage capabilities. They utilized techniques like cyclic voltammetry and impedance spectroscopy to characterize the electrochemical behaviour of $Ta_3N_5$ electrodes. The different studies are reported in the following Table 3.1.

**Table 1. Different Tafel slopes measurements for Substrate and catalyst $Ta_3N_5$.**

| Catalyst | Tafel slope mV/ dec | Electrolytes |
|---|---|---|
| Elemental Pt | 530 | 0.1 M $H_2SO_4$ |
| NiFeOx | 40 | 1.0 M NaOH |
| $Co_3O_4$ | 54 | 1 M KOH |
| RhOx/CoOx | 40 | 0.1 M $Na_2S_2O_8$ |

### 1. Electrocatalytic Methods for Preparation of Catalysts

The preparation of the electrocatalyst for the Oxygen evolution could lead to increase its activity, because its importance in the evolution is very important. There are many methods for the preparation of electrocatalyst as few of them are precipitation method, hydrothermal method, electrochemical methods, sol-gel method, and microwave assisted synthesis.

#### i.Hydrothermal Method

The controlled nanostructure and high purity simple oxides and nano sized spinel can be prepared with this hydrothermal method. The morphology of the nanoparticles can be adjusted the reaction temperature and pressure. The aqueous solution KOH or NaOH are mixed with the metal salts which includes acetate, chloride and nitrate, then this mixture is autoclaved in which the solvent is sealed and heated for several hours to obtain the products [77].

According to the stoichiometric technique, Ferrous ammonium sulphate and nickel sulphate were mixed up, and then this solvent mixture added into the autoclave which is prepared with the Teflon-lined stainless steel at temperature of 150 °C, where oxide is annealed with the help of high temperature and high pressure.

The nanosheets on which Manganese and Cobalt substituted with Iron oxide nanoparticles by Facile hydrothermal method. Solvents are used in this method like ethylene glycol, isopropanol, Ethanol, dimethylformamide (DMF) and tertiary butanol.

#### ii.Solution-phase methods

The preparation of high yield mass production can be done by using this method. This method is also very promising with low temperature for the shape control, surface functionalization and hybridization [111]. One solution phase method for the preparation of $Ta_3N_5$ is the hydrothermal method. This involves the reaction of tantalum precursor and nitrogen source in an aqueous solution under high pressure and temperature. This method has been reported to produce high purity $Ta_3N_5$ with a well-defined morphology and high photocatalytic activity [112]. For instance, reported the preparation of $Ta_3N_5$ using the hydrothermal method. In their study, tantalum ethoxide and urea were used as the precursor and nitrogen source, respectively. The mixture was stirred and heated in an autoclave at 200°C for 24 hours. This study reported a high purity $Ta_3N_5$ product with a specific surface area of 42.8 m2/g and high photocatalytic activity for the degradation of organic pollutants [113]. Similarly, it is reported the preparation of $Ta_3N_5$ using a hydrothermal method with tantalum pentoxide and urea as the precursor and nitrogen source, respectively for the degradation of methylene blue [112].

Solution-phase method in which the different processes which are being takes place like polymerisation, condensation, solvent evaporation and annealing. This method is usually taken for the production of materials on larger commercial scale i.e., industrial scale.

**iii.Sol-gel Method**

Sol-gel method is an environment friendly method for the synthesis of nanomaterials [115]. High purity and high-quality nanoparticles can be synthesized by this method. Sol-gel process involves the transition of a solution system from a liquid sol into a solid phase [116]. That is a sol is converted into gel phase. For the heating treatment the solution placed at hot plate and heating will continue till to the critical temperature where auto combustion takes place and the final gel burnout then we get a fine powder [117]. This is low-cost, simple and reliable way for the synthetization of alloy, composite, ceramic, organic and inorganic sample [118]. It is not time-consuming process, and also it is magnificent stoichiometric controllable method [119]. The material formed highly pure, as multi component, it's a homogenous mixing. At a very low temperature as compared to other techniques auto combustion takes place [120]. The sol-gel method is a popular technique for the preparation of various materials, including $Ta_3N_5$. A sol is prepared by mixing metal precursors with a solvent, followed by hydrolysis and condensation reactions. The resulting gel is then heated to obtain the desired material [121].

Nanosized can be prepared with the help of sol-gel method, because this is a fast, easy and fair methods. Multicomponent systems that is homogenous system works on the low processing and stoichiometric control method has advantages over the other methods [122]. Chelating agents which include $C_6H_8O_7$, $C_{10}H_{16}N_2O_8$, $C_3H_6O_2$, $C_2H_6O_2$, $C_2H_5NO_2$, $CH_3COOH$, Pluronic-123 (P123), or $C_6H_6O_2$ / $CH_2O$ in the metal salts, to form a homogeneous solution. For the obtaining of the final product, calcination is done, like in different studies this sol-gel method for the formation $NiFe_2O_4$, $CoFe_2O_4$, and $CoNiFe_2O_4$ in the oxygen evolution reaction [123].

**iv.Chemical Reduction Method**

The chemical reduction method for the preparation of $Ta_3N_5$ involves the reduction of tantalum pentoxide ($Ta_2O_5$) using ammonia ($NH_3$) gas as the reducing agent. The reaction takes place at high temperature and pressure in a sealed reactor. The $Ta_3N_5$ product is obtained as a black powder. One study that describes the chemical reduction method for the preparation of $Ta_3N_5$ [124].

This the method to make metal nanoparticles, a reducing agent is dissolved in water, often sodium borohydride. Reducing agents are sometimes mixed with stabilizing agents. Absorbance analysis examined the dispersion stability of metal nanoparticles. There are a number of drawbacks that are connected with reducing agents, including their toxicity, increased price, limited capacity to reduce, high costs, and impurities.

**v.Precipitation Method**

The precipitation method for the preparation of $Ta_3N_5$ involves the precipitation of tantalum ions from a solution followed by the thermal treatment of the precipitate to form the nitride. One study by [125] described the preparation of $Ta_3N_5$ by the precipitation method using ammonium bicarbonate as the precipitant. Metal oxide nanoparticles are prepared in this method, which is not inclined for any special equipment, or a complicated process, as it is used to control the particle size and shape, and at the end different constituents are mixed thoroughly in this method [127]. In recent studies, to get the high electrocatalyst cavity, this method is followed as $MnSO_4{\cdot}H_2O$, $CrCl_3$ and $(NH_4)_2Fe(SO_4)_2{\cdot}6H_2O$ along with Manganese ferrites in which Cr was replaced with the Manganese ferrites in which NaOH was added at the end [128].

**vi.Electrochemical Method**

One electrochemical method for the preparation of $Ta_3N_5$ involves the use of Ta metal as the starting material and an electrolyte consisting of $NH_4Cl$ and $NH_4F$. This method was described in a study by [129] who reported the synthesis of $Ta_3N_5$ nanoparticles using a cyclic voltammetry technique. In this method, a Ta electrode is used

as the working electrode and a Pt wire and Ag/AgCl electrode are used as the counter and reference electrodes, respectively [130]. The cyclic voltammetry technique is used to repeatedly apply a potential range of -0.6 V to 0.8 V vs. Ag/AgCl to the Ta electrode, causing the formation of $Ta_3N_5$ nanoparticles on the surface of the electrode. The resulting $Ta_3N_5$ nanoparticles are then collected by ultrasonicating the electrode in water [130]. This study demonstrated that the electrochemical synthesis of $Ta_3N_5$ nanoparticles was highly efficient and could be easily scaled up for large-scale production [130].

**vii. Electrospinning Method**

Electrospinning method is famous for the synthesis of the nanofibers from the polymers, ceramics and polymers [131]. This method has gained much importance in the recent studies, because of, high electrocatalytic activity, mass transformed, and high surface area [132]. A precursor is required to prepare the nanofibers. To be more précised, Electrospinning process is explained with the help of the given Figure 2.1. A high voltage connected syringe is used to load the precursor with a metallic needle. The voltage range usually varies between 5 to 30 kV [133]. Syringe which is ejecting the precursor onto the collector, and leading towards the formation of the nanofibers of the $Ta_3N_5$ on the nonwoven mat. It is also depicted the electrospinning method for the preparation the nanofibers after calcinating solvothermal reaction.

$Ta_3N_5$ is being formed with the help of electrospinning method for various applications, including photocatalysis, water splitting, and energy storage. One study that utilized electrospinning for the preparation of $Ta_3N_5$ [134]. $Ta_3N_5$ nanofibers were prepared using a simple electrospinning technique followed by thermal treatment. The resulting $Ta_3N_5$ nanofibers exhibited excellent photocatalytic activity for the degradation of Rhodamine B under visible light irradiation [135]. The reason behind the excellent photocatalytic activity of the nanofibers is the narrow band gap, for the absorption of visible light photons. Another important logic for the excellent activity is of the high surface area of the electro spun $Ta_3N_5$ fibres [136]. Furthermore, photocatalytic activity can also be increased with the help of nano composition of these fibres with the carbon-based materials or metal nano particles. The last but not the least, operating conditions likewise concentrations, temperature and pH can also further increase the photocatalytic activity [137].

In conclusion, electro spun nanofibers are considered to be the long-term stable and reusability of the materials. Multiple tests have been done to demonstrate the photocatalytic stability by the degradation of the Rhodamine B under the irradiation of the visible light [138].

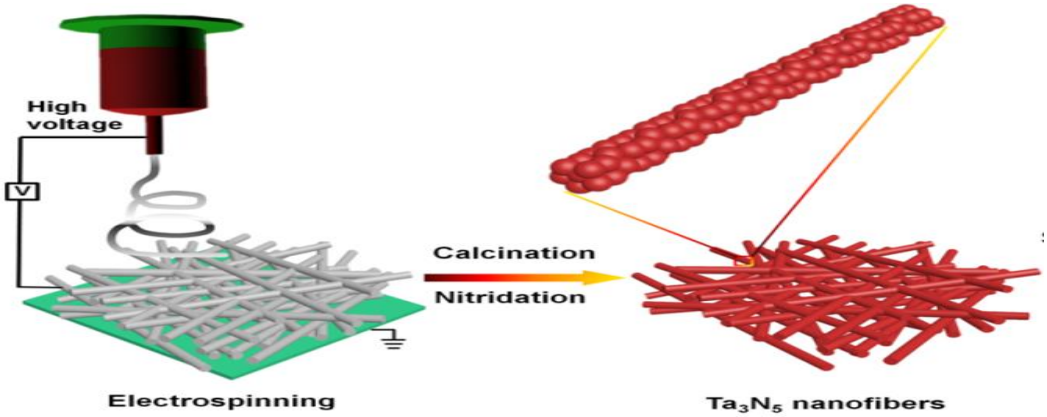


**Figure 4. Schematic diagram for the preparation of $Ta_3N_5$ and $Bi_2WO_6$ [139]. Produced Under common creative license 3.0.**

**Conclusion**

It is concluded from the above reported studies that photoanodic $Ta_3N_5$ has shown promising result for the OER as a critical process. If other metals or non-metals introduced on the surface of the related photoanode $Ta_3N_5$ can increase the oxygen evolution by generating more active sites. The reported non-metals material can increase the OER is $SiO_2$. It is also reported the OER performance can be enhanced by surface modification of the $Ta_3N_5$ as cobalt, nickel, or iron oxide has been found to significantly improve the OER performance of $Ta_3N_5$. In addition, Pt, RuO2, or IrO2 are the co-catalysts are used for the further enhancement of OER. These co-catalysts can effectively promote the charge transfer and reduce the overpotential required for OER.

Overall, it can be concluded that surface modification and co-catalyst deposition are effective strategies to enhance the OER performance of $Ta_3N_5$ and can lead to more efficient water splitting processes for sustainable energy production. However, further research is needed to optimize the synthesis and design of these modified $Ta_3N_5$ catalysts to achieve even better OER activity and stability.

**REFERENCES**

[1] McLinko, R.M.; Sagar, B.V. Space-based solar power generation using a distributed network of satellites and methods for efficient space power transmission. *Proc. SPIE*, **2010**, *7651*, 908–914.

[2] Cheng, W.H.; Richter, M.H.; May, M.M.; Ohlmann, J.; Lackner, D.; Dimroth, F.; Hannappel, T.; Atwater, H. A.; Lewerenz, H. J. Monolithic photoelectrochemical device for direct water splitting with 19% efficiency. *ACS Energy Lett.*, **2018**, *3*(8), 1795–1800.

[3] Rahman, A.; Dargusch, P.; Wadley, D. The political economy of oil supply in Indonesia and the implications for renewable energy development. *Renew. Sustain. Energy Rev.*, **2021**, *144*, 111027.

[4] Zhironkin, S.; Voloshin, A.; Zhironkina, O.; Vöth, S.; Kayachev, G. The principles of sustainable development as a form of structural transformation. *E3S Web Conf.*, **2020**, *174*, 04011.

[5] Iqbal, S.; Khatoon, H.; Pandit, A. H.; Ahmad, S. Recent development of carbon based materials for energy storage devices. *Mater. Sci. Energy Technol.*, **2019**, *2*(3), 417–428.

[6] Yoro, K. O.; Daramola, M. O. $CO_2$ emission sources, greenhouse gases, and the global warming effect. *In Adv.*, **2020**, pp. 3–28.

[7] Brumberg, H. L.; Karr, C. J.; Bole, A.; Ahdoot, S.; Balk, S. J.; Bernstein, A. S.; Byron, L. G.; Landrigan, P. J.; Marcus, S. M.; Nerlinger, A. L.; Pacheco, S. E. Ambient air pollution: health hazards to children. *Pediatrics*, **2021**, *147*(6).

[8] Capitaine, A.; Sciacca, B. Monocrystalline methylammonium lead halide perovskite materials for photovoltaics. *Adv. Mater.*, **2021**, *33*(52), 2102588.

[9] Ram, M.; Aghahosseini, A.; Breyer, C. Job creation during the global energy transition towards 100% renewable power system by 2050. *Technol. Forecast. Soc. Change*, **2020**, *151*, 119682.

[10] Taherahmadi, J.; Noorollahi, Y.; Panahi, M. Toward comprehensive zero energy building definitions: a literature review and recommendations. *Int. J. Sustain. Energy*, **2021**, *40*(2), 120–148.

[11] Bahar, N.H.; Lo, M.; Sanjaya, M.; Van Vianen, J.; Alexander, P.; Ickowitz, A.; Sunderland, T. Meeting the food security challenge for nine billion people in 2050: What impact on forests? *Glob. Environ. Change*, **2020**, *62*, 102056.

[12] Moriarty, P.; Honnery, D. Global renewable energy resources and use in 2050. In Managing Global Warming. *Academic Press*, **2019**, pp. 221–235.

[13] Salkuti, S.R. Emerging and advanced green energy technologies for sustainable and resilient future grid. *Energies*, **2022**, *15*(18), 6667.

[14] Qazi, A.; Hussain, F.; Rahim, N.A.; Hardaker, G.; Alghazzawi, D.; Shaban, K.; Haruna, K. Towards sustainable energy: a systematic review of renewable energy sources, technologies, and public opinions. *IEEE Access*, **2019**, *7*, 63837–63851.

[15] Cook, T.R.; Dogutan, D.K.; Reece, S.Y.; Surendranath, Y.; Teets, T.S.; Nocera, D.G. Solar energy supply and storage for the legacy and nonlegacy worlds. *Chem. Rev.*, **2010**, *110*(11), 6474-6502.

[16] Grushevskaya, S.; Belyanskaya, I.; Kozaderov, O. Approaches for modifying oxide-semiconductor materials to increase the efficiency of photocatalytic water splitting. *Materials*, **2022**, *15*(14), 4915.

[17] Kong, W.; Zhang, X.; Liu, S.; Zhou, Y.; Chang, B.; Zhang, S.; Fan, H.; Yang, B. N doped carbon dot modified $WO_3$ nanoflakes for efficient photoelectrochemical water oxidation. *Adv. Mater*, **2019**, *6*(1), 1801653.

[18] Luo, X.; Ma, X.; Xu, Y.F.; Feng, Z.K.; Du, W.P.; Wang, R.Z.; Li, M. Solar water heating system. *In Handb. Energy Syst. Green Build.*, **2018**, pp. 1–51.

[19] De Crisci, A.G.; Moniri, A.; Xu, Y. Hydrogen from hydrogen sulfide: towards a more sustainable hydrogen economy. *Int. J. Hydrogen Energy*, **2019**, *44*(3), 1299–1327.

[20] Anwar, S.; Khan, F.; Zhang, Y.; Djire, A. Recent development in electrocatalysts for hydrogen production through water electrolysis. *Int. J. Hydrogen Energy*, **2021**, *46*(63), 32284–32317.

[21] Toivari, M.; Nygård, Y.; Kumpula, E.P.; Vehkomäki, M.L.; Benčina, M.; Valkonen, M.; Maaheimo, H.; Andberg, M.; Koivula, A.; Ruohonen, L.; Penttilä, M. Metabolic engineering of Saccharomyces cerevisiae for bioconversion of D-xylose to D-xylonate. *Metab. Eng.*, **2012**, *14*(4), 427–436.

[22] Venkatesan, S.V.; Nandy, A.; Karan, K.; Larter, S.R.; Thangadurai, V. Recent advances in the unconventional design of electrochemical energy storage and conversion devices. Electrochem. *Energy Rev.*, **2022**, *5*(4), 16.

[23] Akram, R.; Chen, F.; Khalid, F.; Ye, Z.; Majeed, M.T. Heterogeneous effects of energy efficiency and renewable energy on carbon emissions: Evidence from developing countries. *J. Clean. Prod.*, **2020**, *247*, 119122.

[24] Marschall, R. 50 years of materials research for photocatalytic water splitting. *Eur. J. Inorg. Chem.*, **2021**, (25), 2435–2441.

[25] Chen, F.Y.; Wu, Z.Y.; Adler, Z.; Wang, H. Stability challenges of electrocatalytic oxygen evolution reaction: From mechanistic understanding to reactor design. *Joule*, **2021**, *5*(7), 1704–1731.

[26] Seh, Z.W.; Kibsgaard, J.; Dickens, C.F.; Chorkendorff, I.B.; Nørskov, J.K.; Jaramillo, T.F. Combining theory and experiment in electrocatalysis: Insights into materials design. *Sci.*, **2017**, *355*(6321), 4998.

[27] Han, L.; Dong, S.; Wang, E. Transition-metal (Co, Ni, and Fe)-based electrocatalysts for the water oxidation reaction. *Adv. Mater.*, **2016**, *28*(42), 9266–9291.

[28] Tao, H.B.; Xu, Y.; Huang, X.; Chen, J.; Pei, L.; Zhang, J.; Chen, J.G.; Liu, B. A general method to probe oxygen evolution intermediates at operating conditions. *Joule*, **2019**, *3*(6), 1498–1509.

[29] Tyburski, R.; Liu, T.; Glover, S. D.; Hammarström, L. Proton-coupled electron transfer guidelines, fair and square. *J. Am. Chem. Soc.*, **2021**, *143*(2), 560–576.

[30] Yin, M.; Miao, H.; Hu, R.; Sun, Z.; Li, H. Manganese dioxides for oxygen electrocatalysis in energy conversion and storage systems over full pH range. *J. Power Sources*, **2021**, *494*, 229779.

[31] Gong, M.; Dai, H. A mini review of NiFe-based materials as highly active oxygen evolution reaction electrocatalysts. *Nano Res.*, **2015**, *8*(1), 23–39.

[32] Wang, A. L.; Dong, Y. T.; Li, M.; Liang, C.; Li, G. R. In situ derived $NixFe_{1-x}OOH$/NiFe/$NixFe_{1-x}OOH$ nanotube arrays from NiFe alloys as efficient electrocatalysts for oxygen evolution. *ACS Appl.*, **2017**, *9*(40), 34954–34960.

[33] Eo, T.; Katsuki, T.; Berber, M.R.; Zahran, Z.N.; Mohamed, E.A.; Tsubonouchi, Y.; Alenad, A.M.; Althubiti, N.A.; Yagi, M. Handy protocol of nitrogen-doped $BiVO_4$ photoanode for visible light-driven water oxidation. *ACS Appl. Energy Mater.*, **2021**, *4*(4), 2983–2989.

[34] Kumari, M.G.C.M.; Perera, C.S.; Dassanayake, B.S.; Dissanayake, M.A.K.L.; Senadeera, G.K.R. Highly efficient plasmonic dye-sensitized solar cells with silver nanowires and $TiO_2$ nanofibres incorporated multi-layered photoanode. *Electrochim. Acta*, **2019**, *298*, 330–338.

[35] Chen, Y.; Li, H.; Ma, Q.; Che, Q.; Wang, J.; Wang, G.; Yang, P. Morphology-controlled porous $\alpha$-$Fe_2O_3$/$SnO_2$ nanorods with uniform surface heterostructures and their enhanced acetone gas-sensing properties. *Mater. Lett.*, **2018**, *211*, 212–215.

[36] Saddique, Z.; Imran, M.; Javaid, A.; Kanwal, F.; Latif, S.; dos Santos, J.C.S.; Kim, T.H.; Boczkaj, G. Bismuth-based nanomaterials-assisted photocatalytic water splitting for sustainable hydrogen production. *Int. J. Hydrogen Energy*, **2024**, *52*, 594–611.

[37] Ayappan, C.; Jayaraman, V.; Palanivel, B.; Pandikumar, A.; Mani, A. Facile preparation of novel $Sb_2S_3$ nanoparticles/rod-like $\alpha$-$Ag_2WO_4$ heterojunction photocatalysts: continuous modulation of band structure towards the efficient removal of organic contaminants. *Sep. Purif. Technol.*, **2020**, *236*, 116302.

[38] Sayed, M.S.; Mohapatra, D.; Baynosa, M.L.; Shim, J.J. Three-dimensional core-shell heterostructure of tungsten trioxide/bismuth molybdate/cobalt phosphate for enhanced photoelectrochemical water splitting. *J. Colloid Interface Sci.*, **2021**, *598*, 348–357.

[39] Mehta, A.; Mishra, A.; Basu, S.; Shetti, N.P.; Reddy, K.R.; Saleh, T.A.; Aminabhavi, T. M. Band gap tuning and surface modification of carbon dots for sustainable environmental remediation and photocatalytic hydrogen production. A review. *J. Environ. Manage*, **2019**, *250*, 109486.

[40] Hara, M.; Chiba, E.; Ishikawa, A.; Takata, T.; Kondo, J.N.; Domen, K. $Ta_3N_5$ and TaON thin films on Ta foil: Surface composition and stability. *J. Phys. Chem. B*, **2003**, *107*(48), 13441–13445.

[41] Chen, S.; Wang, L.W. Thermodynamic oxidation and reduction potentials of photocatalytic semiconductors in aqueous solution. *Chem. Mater.*, **2012**, *24*(18), 3659–3666.

[42] Wagner, L.I.; Sirotti, E.; Brune, O.; Grötzner, G.; Eichhorn, J.; Santra, S.; Munnik, F.; Olivi, L.; Pollastri, S.; Streibel, V.; Sharp, I.D. Defect engineering of $Ta_3N_5$ photoanodes: enhancing charge transport and photoconversion efficiencies via Ti doping. *Adv. Funct. Mater.*, **2024**, *34*(4), 2306539.

[43] Takanabe, K. Photocatalytic water splitting: quantitative approaches toward photocatalyst by design. *ACS Catal.*, **2017**, *7*(11), 8006–8022.

[44] Jing, T.; Dai, Y.; Ma, X.; Wei, W.; Huang, B. Effects of intrinsic defects and extrinsic doping on the electronic and photocatalytic properties of $Ta_3N_5$. *RSC Adv.*, **2015**, *5*(73), 59390–59397.

[45] Smith, R.D.; Prévot, M.S.; Fagan, R.D.; Zhang, Z.; Sedach, P.A.; Siu, M.K.J.; Trudel, S.; Berlinguette, C.P. Photochemical route for accessing amorphous metal oxide materials for water oxidation catalysis. *Sci.*, **2013**, *340*(6128), 60–63.

[46] Chun, W.J.; Ishikawa, A.; Fujisawa, H.; Takata, T.; Kondo, J.N.; Hara, M.; Kawai, M.; Matsumoto, Y.; Domen, K. Conduction and valence band positions of $Ta_2O_5$, TaON, and $Ta_3N_5$ by UPS and electrochemical methods. *J. Phys. Chem. B*, **2003**, *107*(8), 1798–1803.

[47] Brown, S. Ambient ammonia synthesis via microwave-catalytic materials and plasma chemistry. Doctoral dissertation, West Virginia University. *Sci.*, **2015**, *12*, 229-224.

[48] Nian, L.; Kan, Y.; Wang, H.; Gao, K.; Xu, B.; Rong, Q.; Wang, R.; Wang, J.; Liu, F.; Chen, J.; Zhou, G. Ternary non-fullerene polymer solar cells with 13.51% efficiency and a record-high fill factor of 78.13%. *Energy Environ. Sci.*, **2018**, *11*(12), 3392–3399.

[49] Ziani, A.; Nurlaela, E.; Dhawale, D.S.; Silva, D.A.; Alarousu, E.; Mohammed, O.F.; Takanabe, K. Carrier dynamics of a visible-light-responsive $Ta_3N_5$ photoanode for water oxidation. *Phys. Chem. Chem. Phys.*, **2015**, *17*(4), 2670–2677.

[50] He, Y.; Thorne, J.E.; Wu, C.H.; Ma, P.; Du, C.; Dong, Q.; Guo, J.; Wang, D. What limits the performance of $Ta_3N_5$ for solar water splitting? *Chem*, **2016**, *1*(4), 640–655.

[51] AlOtaibi, B.; Harati, M.; Fan, S.; Zhao, S.; Nguyen, H.P.T.; Kibria, M. G.; Mi, Z. High efficiency photoelectrochemical water splitting and hydrogen generation using GaN nanowire photoelectrode. *Nanotechnology*, **2013**, *24*(17), 175401.

[52] Zhong, M.; Hisatomi, T.; Sasaki, Y.; Suzuki, S.; Teshima, K.; Nakabayashi, M.; Shibata, N.; Nishiyama, H.; Katayama, M.; Yamada, T.; Domen, K. Highly active GaN-stabilized $Ta_3N_5$ thin-film photoanode for solar water oxidation. *Angew. Chem.*, **2017**, *129*(17), 4817–4821.

[53] Nurlaela, E.; Shinagawa, T.; Qureshi, M.; Dhawale, D. S.; Takanabe, K. Temperature dependence of electrocatalytic and photocatalytic oxygen evolution reaction rates using NiFe oxide. *ACS Catal.*, **2016**, *6*(3), 1713–1722.

[54] Saraswat, S.K.; Rodene, D.D.; Gupta, R.B. Recent advancements in semiconductor materials for photoelectrochemical water splitting for hydrogen production using visible light. *Renew. Sustain. Energy Rev.*, **2018**, *89*, 228–248.

[55] Ma, M.; Huang, Y.; Liu, J.; Liu, K.; Wang, Z.; Zhao, C.; Qu, S.; Wang, Z. Engineering the photoelectrochemical behaviors of ZnO for efficient solar water splitting. *J. Semicond.*, **2020**, *41*(9), 091702.

[56] Xu, X.T.; Pan, L.; Zhang, X.; Wang, L.; Zou, J.J. Rational design and construction of cocatalysts for semiconductor-based photo-electrochemical oxygen evolution: a comprehensive review. *Adv. Sci.*, **2019**, *6*(2), 1801505.

[57] Gonçalves, J.M.; da Silva, M.I.; Angnes, L.; Araki, K. Vanadium-containing electro and photocatalysts for the oxygen evolution reaction: a review. *J. Mater. Chem. A*, **2020**, *8*(5), 2171–2206.

[58] Chong, R.; Wang, Z.; Lv, J.; Rong, J.; Zhang, L.; Jia, Y.; Wang, L.; Chang, Z.; Wang, X. A hybrid CoOOH-rGO/$Fe_2O_3$ photoanode with spatial charge separation and charge transfer for efficient photoelectrochemical water oxidation. *J. Catal.*, **2021**, *399*, 170–181.

[59] Yuan, C.; Yin, H.; Li, J.; Zhang, Y.; Chen, H.; Xiao, D.; Wang, Q.; Zhang, Y.; Xue, Q.K. Light-induced CoOX surface reconstruction in hollow heterostructure for durable photocatalytic seawater splitting. *Nat. Commun.*, **2025**, *16*(1), p.6607.

[60] Alex, C.; Sarma, S.C.; Peter, S.C.; John, N.S. Competing effect of $Co^{3+}$ reducibility and oxygen-deficient defects toward high oxygen evolution activity in $Co_3O_4$ systems in alkaline medium. *ACS Appl. Energy Mater.*, **2020**, *3*(6), 5439–5447.

[61] Wang, Y.; Wang, T.; Arandiyan, H.; Song, G.; Sun, H.; Sabri, Y.; Zhao, C.; Shao, Z.; Kawi, S. Advancing catalysts by stacking fault defects for enhanced hydrogen production: a review. *Adv. Mater.*, **2024**, *36*(21), 2313378.

[62] Hajibabaei, H.; Zandi, O.; Hamann, T.W. Tantalum nitride films integrated with transparent conductive oxide substrates via atomic layer deposition for photoelectrochemical water splitting. *Chem. Sci.*, **2016**, 7(11), 6760–6767.

[63] Li, Z.; Dewulf, B.; Binnemans, K. Nonaqueous solvent extraction for enhanced metal separations: concept, systems, and mechanisms. *Ind. Eng. Chem. Res.*, **2021**, *60*(48), 17285–17302.

[64] Zhao, Y. $WO_3$ for photoelectrochemical water splitting: from plain films to 3D architectures. In Photoelectrochemical Solar Fuel Production: From Basic Principles to Advanced Devices; Li, Y., Ed.; *Springer*, **2020**, pp. 345–373.

[65] Pihosh, Y.; Minegishi, T.; Nandal, V.; Higashi, T.; Katayama, M.; Yamada, T.; Sasaki, Y.; Seki, K.; Suzuki, Y.; Nakabayashi, M.; Sugiyama, M. $Ta_3N_5$-nanorods enabling highly efficient water oxidation via advantageous light harvesting and charge collection. *Energy Environ. Sci.*, **2020**, *13*(5), 1519–1530.

[66] Peng, Z.; Jiang, Y.; Xiao, Y.; Xu, H.; Zhang, W.; Ni, L. $CdIn_2S_4$ surface-decorated $Ta_3N_5$ core-shell heterostructure for improved spatial charge transfer: in-situ growth, synergistic effect and efficient dual-functional photocatalytic performance. *Appl. Surf. Sci.*, **2019**, *487*, 1084–1095.

[67] Zhong, Y.; Peng, C.; He, Z.; Chen, D.; Jia, H.; Zhang, J.; Ding, H.; Wu, X. Interface engineering of heterojunction photocatalysts based on 1D nanomaterials. *Catal. Sci. Technol.*, **2021**, *11*(1), 27–42.

[68] Lee, S.J.; Jang, H. Recent advances in nanoflowers: compositional and structural diversification for potential applications. *Nanoscale Adv.*, **2023**, *5*(19), pp.5165–5213.

[69] Liu, Y.; Sun, Z.; Hu, Y.H. Bimetallic cocatalysts for photocatalytic hydrogen production from water. *Chem. Eng. J.*, **2021**, *409*, 128250.

[70] Otieno, S.; Lanterna, A.E.; Mack, J.; Derese, S.; Amuhaya, E.K.; Nyokong, T.; Scaiano, J.C. Solar driven photocatalytic activity of porphyrin sensitized $TiO_2$: experimental and computational studies. *Molecules*, **2021**, *26*(11), 3131.

[71] Heli, H.; Rahi, A. Synthesis and applications of nanoflowers. *Recent Pat. Nanotechnol.*, **2016**, *10*(2), pp.86–115.

[72] Grabowska, E.; Marchelek, M.; Paszkiewicz-Gawron, M.; Zaleska-Medynska, A. Metal oxide photocatalysts. In Handbook of Smart Photocatalytic Materials; S. S. Umrao, Ed.; *Springer*, **2018**; pp. 1–32.

[73] Dong, Y.; Ai, F.; Sun-Waterhouse, D.; Murai, K.I.; Moriga, T.; Waterhouse, G.I. Optical and photocatalytic properties of three-dimensionally ordered macroporous $Ta_2O_5$ and $Ta_3N_5$ inverse opals. *Chem. Mater.*, **2023**, **35**(19), 8281–8300.

[74] Chauhan, P.S.; Kant, R.; Rai, A.; Gupta, A.; Bhattacharya, S. Facile synthesis of ZnO/GO nanoflowers over Si substrate for improved photocatalytic decolorization of MB dye and industrial wastewater under solar irradiation. *Mater. Sci. Semicond. Process.*, **2019**, *89*, 6–17.

[75] Jiang, H.; Dai, H.; Meng, X.; Ji, K.; Zhang, L.; Deng, J. Porous olive-like $BiVO_4$: alcohol-hydrothermal preparation and excellent visible-light-driven photocatalytic performance for the degradation of phenol. *Appl. Catal. B Environ.*, **2011**, *105*(3–4), 326–334.

[76] Jafari, T.; Moharreri, E.; Amin, A.S.; Miao, R.; Song, W.; Suib, S.L. Photocatalytic water splitting the untamed dream: a review of recent advances. *Molecules*, **2016**, *21*(7), p.900.

[77] Du, J.; Chen, C.; Cheng, F.; Chen, J. Rapid synthesis and efficient electrocatalytic oxygen reduction/evolution reaction of $CoMn_2O_4$ nanodots supported on graphene. *Inorg. Chem.*, **2015**, *54*(11), 5467–5474.

[78] Song, S.; Xing, Z.; Zhao, H.; Li, Z.; Zhou, W. Recent advances in bismuth-based photocatalysts: environment and energy applications. *Green Energy Environ.*, **2023**, *8*(5), 1232–1264.

[79] Hayat, A.; Sohail, M.; Anwar, U.; Taha, T.A.; Qazi, H.I.A.; Amina; Ajmal, Z.; Al-Sehemi, A.G.; Algarni, H.; Al-Ghamdi, A.A.; Amin, M.A. A targeted review of current progress, challenges and future perspective of g-$C_3N_4$ based hybrid photocatalyst toward multidimensional applications. *Chem. Rec.*, **2023**, *23*(1), e202200143.

[80] Cecconet, D.; Sturini, M.; Malavasi, L.; Capodaglio, A.G. Graphitic carbon nitride as a sustainable photocatalyst material for pollutants removal: state-of-the-art, preliminary tests and application perspectives. *Materials*, **2021**, *14*(23), 7368.

[81] Ikram, M.; Raza, A.; Ahmad, S.O.A.; Ashfaq, A.; Akbar, M. U.; Imran, M.; Dilpazir, S.; Khan, M.; Khan, Q.; Maqbool, M. Solar-triggered engineered 2D materials for environmental remediation: status and future insights. *Adv. Mater. Interfaces*, **2023**, *10*(11), 2202172.

[82] Gujral, H.S.; Singh, G.; Baskar, A.V.; Guan, X.; Geng, X.; Kotkondawar, A.V.; Rayalu, S.; Kumar, P.; Karakoti, A.; Vinu, A. Metal nitride-based nanostructures for electrochemical and photocatalytic hydrogen production. *Sci. Technol. Adv. Mater.*, **2022**, *23*(1), 76–119.

[83] Rodrigues, B.S.; Branco, C.M.; Corio, P.; Souza, J.S. Controlling bismuth vanadate morphology and crystalline structure through optimization of microwave-assisted synthesis conditions. *Cryst. Growth Des.*, **2020**, *20*(6), 3673–3685.

[84] Fu, J.; Skrabalak, S.E. Aerosol synthesis of shape-controlled template particles: a route to $Ta_3N_5$ nanoplates and octahedra as photocatalysts. *J. Mater. Chem. A*, **2016**, *4*(21), pp.8451–8457.

[85] Lou, Z.; Yang, Y.; Wang, Y.; Qin, C.; Liang, R.; Wang, Y.; Ye, Z.; Zhu, L. $LaCl_3$ flux mediated $Ta_3N_5$ planar photoanode for solar water oxidation. *Chem. Eng. J.*, **2020**, *396*, 125161.

[86] Isachenko, A.I.; Apyari, V.V.; Melekhin, A.O.; Garshev, A.V.; Volkov, P. A.; Dmitrienko, S.G. Borohydride-modified polyurethane foam: a new form of a widely known reducing agent in synthesis of metal nanoparticles for sensing applications. *Appl. Nanosci.*, **2020**, *10*(4), 1023–1033.

[87] Patra, D.; El Kurdi, R. Curcumin as a novel reducing and stabilizing agent for the green synthesis of metallic nanoparticles. *Green Chem. Lett. Rev.*, **2021**, *14*(3), 474–487.

[88] Kumari, S.C.; Dhand, V.; Padma, P.N. Green synthesis of metallic nanoparticles: a review. In Green Synthesis in Nanomedicine and Human Health; Kalia, S., Ed.; *Academic Press*, **2021**, pp. 259–281.

[89] Mushtaq, M.A.; Kumar, A.; Yasin, G.; Arif, M.; Tabish, M.; Ibraheem, S.; Cai, X.; Ye, W.; Fang, X.; Saad, A.; Zhao, J. 3D interconnected porous Mo-doped $WO_3$@CdS hierarchical hollow heterostructures for efficient photoelectrochemical nitrogen reduction to ammonia. *Appl. Catal. B Environ.*, **2022**, *317*, 121711.

[90] Farrukh, S.; Fan, X.; Mustafa, K.; Hussain, A.; Ayoub, M.; Younas, M. Nanotechnology and the generation of sustainable hydrogen. *Springer Nature.*, **2020**, 223-224.

[91] Kustiyah, E.; Naidir, F.; Nuraliyah, A.; Hasaya, H.; Ismaniah, I. Membangun persepsi generasi muda dalam menjaga lingkungan dengan cara literasi Think Green dengan komposter. J. Appr. Technol. *Community Serv.*, **2024**, *5*(2), 129–136.

[92] Luo, Y.; Wu, Y.; Huang, C.; Menon, C.; Feng, S.P.; Chu, P.K. Plasma modified and tailored defective electrocatalysts for water electrolysis and hydrogen fuel cells. *Eco. Mat*, **2022**, *4*(4), e12197.

[93] Wang, Q.; Zhang, L.; Li, B.; Zhu, H.; Shi, J. 3D interconnected nanoporous $Ta_3N_5$ films for photoelectrochemical water splitting: thickness-controlled synthesis and insights into stability. *Sci. China Mater.*, **2021**, *64*(8), 1876–1888.

[94] Alex, C.; Sarma, S.C.; Peter, S.C.; John, N.S. Competing effect of $Co^{3+}$ reducibility and oxygen-deficient defects toward high oxygen evolution activity in $Co_3O_4$ systems in alkaline medium. *ACS Appl. Energy Mater.*, **2020**, *3*(6), 5439–5447.

[95] Zhu, G.; Yu, X.; Xie, F.; Feng, W. Ultraviolet light assisted heterogeneous Fenton degradation of tetracycline based on polyhedral $Fe_3O_4$ nanoparticles with exposed high-energy {110} facets. *Appl. Surf. Sci.*, **2019**, *485*, 496–505.

[96] Rafique, M.; Mubashar, R.; Irshad, M.; Gillani, S.S.A.; Tahir, M.B.; Khalid, N.R.; Yasmin, A.; Shehzad, M.A. A comprehensive study on methods and materials for photocatalytic water splitting and hydrogen production as a renewable energy resource. *J. Inorg. Organomet. Polym. Mater.*, **2020**, *30*(10), 3837–3861.

[97] Khanal, V.; Irani, R.; Fiechter, S.; Abdi, F.F.; Subramanian, V.R. The photoelectrochemical and photocatalytic properties of tantalum oxide and tantalum nitride. *J. Electrochem. Soc.*, **2019**, *166*(5), H3294.

[98] Zhang, Q.; Gao, L. $Ta_3N_5$ nanoparticles with enhanced photocatalytic efficiency under visible light irradiation. *Langmuir,* **2004**, *20*(22), pp.9821–9827.

[99] Zareef, F.; Rashid, M.; Ahmadini, A.A.H.; Alshahrani, T.; Kattan, N.A.; Laref, A. Optoelectronic, thermoelectrical, and mechanical properties of $CdLu_2X_4$ (X = S, Se) using first-principles calculations for energy harvesting applications. *Mater. Sci. Semicond. Process*, **2021**, *127*, 105695.

[100] Xiao, J.; Vequizo, J.J.M.; Hisatomi, T.; Rabeah, J.; Nakabayashi, M.; Wang, Z.; Xiao, Q.; Li, H.; Pan, Z.; Krause, M.; Yin, N. Simultaneously tuning the defects and surface properties of $Ta_3N_5$ nanoparticles by Mg–Zr codoping for significantly accelerated photocatalytic $H_2$ evolution. *J. Am. Chem. Soc.*, **2021**, *143*(27), 10059–10064.

[101] Yuan, X.; Floresyona, D.; Aubert, P.H.; Bui, T.T.; Remita, S.; Ghosh, S.; Brisset, F.; Goubard, F.; Remita, H. Photocatalytic degradation of organic pollutant with polypyrrole nanostructures under UV and visible light. *Appl. Catal. B Environ.*, **2019**, *242*, 284–292.

[102] Munusamy, S.; Sivaranjan, K.; Sabhapathy, P.; Ramesh, P.S.; Narayanan, V.; Mohammad, F.; Sagadevan, S. Electrochemical and photocatalytic studies of Ta3N5–TaON–PEDOT–PANI nanohybrids. *Chem. Phys. Lett.*, **2021**, 780, 138947.

[103] Ismael, M. A review on graphitic carbon nitride (g-C3N4) based nanocomposites: synthesis, categories, and their application in photocatalysis. *J. Alloys Compd.*, **2020**, *846*, 156446.

[104] Yuliati, L.; Yang, J.H.; Wang, X.; Maeda, K.; Takata, T.; Antonietti, M.; Domen, K. Highly active tantalum(V) nitride nanoparticles prepared from a mesoporous carbon nitride template for photocatalytic hydrogen evolution under visible light irradiation. *J. Mater. Chem.*, **2010**, *20*(21), 4295–4298.

[105] Hayat, A.; Sohail, M.; Ali, H.; Taha, T.A.; Qazi, H.I.A.; Ur Rahman, N.; Ajmal, Z.; Kalam, A.; Al-Sehemi, A.G.; Wageh, S.; Amin, M.A. Recent advances and future perspectives of metal-based electrocatalysts for overall electrochemical water splitting. *Chem. Rec.*, **2023**, *23*(2), e202200149.

[106] Nurlaela, E.; Wang, H.; Shinagawa, T.; Flanagan, S.; Ould-Chikh, S.; Qureshi, M.; Mics, Z.; Sautet, P.; Le Bahers, T.; Canovas, E.; Bonn, M. Enhanced kinetics of hole transfer and electrocatalysis during photocatalytic oxygen evolution by cocatalyst tuning. *ACS Catal.*, **2016**, *6*(7), 4117–4126.

[107] Faraji, S.; Ani, F.N. Microwave-assisted synthesis of metal oxide/hydroxide composite electrodes for high power supercapacitors a review. *J. Power Sources*, **2014**, *263*, 338–360.

[108] Vazhayil, A.; Vazhayal, L.; Thomas, J.; Thomas, N. A comprehensive review on the recent developments in transition metal-based electrocatalysts for oxygen evolution reaction. *Appl. Surf. Sci. Adv.*, **2021**, *6*, 100184.

[109] Kawase, Y.; Higashi, T.; Obata, K.; Sasaki, Y.; Katayama, M.; Domen, K.; Takanabe, K. Interfacial design of a Ta3N5 thin-film photoanode for highly stable oxygen evolution over a wide pH range. ACS *Sustain. Chem. Eng.*, **2022**, *10*(45), 14705–14714.

[110] Dourado, A.H. Electric double layer: the good, the bad, and the beauty. *Electrochem*, **2022**, *3*(4), 789–808.

[111] Andrew, J.J.; Dhakal, H.N. Sustainable biobased composites for advanced applications: recent trends and future opportunities a critical review. *Compos. Part C Open Access*, **2022**, *7*, 100220.

[112] Khan, S.; Zapata, M.J.; Baptista, D.L.; Gonçalves, R.V.; Fernandes, J.A.; Dupont, J.; Santos, M.J.; Teixeira, S.R. Effect of oxygen content on the photoelectrochemical activity of crystallographically preferred oriented porous Ta3N5 nanotubes. *J. Phys. Chem. C*, **2015**, *119*(34), 19906–19914.

[113] Alahmadi, N. Recent progress in photocatalytic removal of environmental pollution hazards in water using nanostructured materials. *Separations*, **2022**, *9*(10), 264.

[114] Wang, X.; Ahmad, M.; Sun, H. Three-dimensional ZnO hierarchical nanostructures: solution phase synthesis and applications. *Materials*, **2017**, *10*(11), 1304.

[115] Shafiee, P.; Nafchi, M.R.; Eskandarinezhad, S.; Mahmoudi, S.; Ahmadi, E. Sol-gel zinc oxide nanoparticles: advances in synthesis and applications. *Synth. Sinter.*, **2021**, *1*(4), 242–254.

[116] Bokov, D.; Turki Jalil, A.; Chupradit, S.; Suksatan, W.; Javed Ansari, M.; Shewael, I. H.; Valiev, G.H.; Kianfar, E. Nanomaterial by sol-gel method: synthesis and application. *Adv. Mater. Sci. Eng.*, **2021**, (1), 5102014.

[117] Yuan, H.; Restuccia, F.; Richter, F.; Rein, G. A computational model to simulate self-heating ignition across scales, configurations, and coal origins. *Fuel*, **2019**, *236*, 1100–1109.

[118] Rane, A.V.; Kanny, K.; Abitha, V.K.; Thomas, S. Methods for synthesis of nanoparticles and fabrication of nanocomposites. *In Synthesis of Inorganic Nanomaterials*, **2018**, pp. 121–139.

[119] Shi, Z.; Zhao, Q.; Guo, B.; Ji, T.; Wang, H. A review on processing polycrystalline magnesium aluminate spinel ($MgAl_2O_4$): Sintering techniques, material properties and machinability. *Materials*, **2020**, *193*, 108858.

[120] Goktas, S.; Goktas, A.J. A comparative study on recent progress in efficient ZnO based nanocomposite and heterojunction photocatalysts: A review. *J. Alloys Compd.*, **2021**, *863*, 158734.

[121] Serhan, M.; Jackemeyer, D.; Long, M.; Sprowls, M.; Perez, I.D.; Maret, W.; Chen, F.; Tao, N.; Forzani, E. Total iron measurement in human serum with a novel smartphone-based assay. *J. Transl. Eng. Health Med.*, **2020**, *8*, 1–9.

[122] Tahir, M.; Pan, L.; Idrees, F.; Zhang, X.; Wang, L.; Zou, J.J.; Wang, Z.L. Electrocatalytic oxygen evolution reaction for energy conversion and storage: A comprehensive review. *Nano Energy*, **2017**, *37*, 136–157.

[123] Zhang, Z.; Zhou, D.; Wu, X.; Bao, X.; Liao, J.; Wen, M. Synthesis of LaO.2SrO.8CoO3 and its electrocatalytic activity for oxygen evolution reaction in alkaline solution. *Int. J. Hydrogen Energy*, **2019**, *44*(14), 7222–7227.

[124] Kędziorski, A.; Smentek, L. New parametrization of spectra of Nd3+ and Sm3+ in glasses. *J. Alloys Compd.*, **2008**, *451*(1–2), 686–690.

[125] Chi, R.A.; Zhou, Z.; Xu, Z.; Hu, Y.; Zhu, G.; Xu, S. Solution-chemistry analysis of ammonium bicarbonate consumption in rare-earth-element precipitation. *Metall. Mater. Trans. B*, **2003**, *34*(5), 611–617.

[126] Xiao, Y.; Zhang, W.; Xing, Q.; Feng, X.; Jiang, Y.; Gao, Y.; Xu, H.; Zhang, J.; Ni, L.; Liu, Z. Eco-friendly synthesis of core/shell ZnIn2S4/Ta3N5 heterojunction for strengthened dual-functional photocatalytic performance. *Int. J. Hydrog. Energy*, **2020**, *45*(55), 30341–30356.

[127] Singh, R.N.; Singh, N.K.; Singh, J.P.; Balaji, G.; Gajbhiye, N.S. Effect of partial substitution of Cr on electrocatalytic properties of formula not shown towards formula not shown-evolution in alkaline medium. *Int. J. Hydrog. Energy*, **2006**, *31*(6), 701–707.

[128] Naz, S.; Durrani, S.K.; Mehmood, M.; Nadeem, M. Hydrothermal synthesis, structural and impedance studies of nanocrystalline zinc chromite spinel oxide material. *Journal of Saudi Chemical Society*, **2016**, *20*(5), pp.585–593.

[129] Jiang, X.; Wang, B.; Luo, L.; Li, W.; Zhou, J.; Chen, H. Electrical properties of (1−x)(Bi0.5Na0.5)TiO3–xKNbO3 lead-free ceramics. *Journal of Solid State Chemistry*, **2014**, *213*, pp.72–78.

[130] Yu, H.; Shen, X.; Tan, W.; Zhang, M.; Lv, J.; Yang, L.; Zhong, J.; He, G.; Sun, Z. Low temperature strategy for the synthesis of Ta3N5 and electrochemical deposition of Ag3PO4 to modify TiO2 as an advanced photoelectrocatalyst for oxygen evolution reactions. *Electrochim. Acta*, **2022**, *430*, p. 140862.

[131] Chronakis, I.S. Novel nanocomposites and nanoceramics based on polymer nanofibers using electrospinning process. A review. *J. Mater. Process. Technol.*, **2005**, *167*, pp.283-293.

[132] Anantharaj, S., Karthik, P.E.; Noda, S. The significance of properly reporting turnover frequency in electrocatalysis research. *Angew. Chem. Int. Ed.*, **2021**, *60*(43), pp.23051–23067.

[133] Li, Y.; Zhu, J.; Cheng, H.; Li, G.; Cho, H.; Jiang, M.; Gao, Q.; Zhang, X. Developments of advanced electrospinning techniques: A critical review. *Adv. Mater. Technol.*, **2021**, *6*(11), p.2100410.

[134] Li, S.; Chen, J.; Hu, S.; Wang, H.; Jiang, W.; Chen, X. Facile construction of novel $Bi_2WO_6/Ta_3N_5$ Z-scheme heterojunction nanofibers for efficient degradation of harmful pharmaceutical pollutants. *Chem. Eng. J.*, **2020**, *402*, p.126165.

[135] Gudipati, T.; Zaman, M.B.; Singh, P.; Poolla, R. Enhanced photocatalytic activity of biogenically synthesized CuO nanostructures against xylenol orange and rhodamine B dyes. *Inorg. Chem. Commun.*, **2021**, *130*, p.108677.

[136] Can, F.; Courtois, X.; Duprez, D. Tungsten-based catalysts for environmental applications. *Catal.*, **2021**, *11*(6), p.703.

[137] Ismael, M. Latest progress on the key operating parameters affecting the photocatalytic activity of $TiO_2$-based photocatalysts for hydrogen fuel production: A comprehensive review. *Fuel*, **2023**, *303*, p.121207.

[138] Martell, M.B.; Linton-Reid, K.; Chen, M.; Aboagye, E.O. Radiomics for lung cancer diagnosis, management, and future prospects. *Clin. Radiol.*, **2025**, p.106926.

[139] Li, S.; Chen, J.; Hu, S.; Wang, H.; Jiang, W.; Chen, X. Facile construction of novel $Bi_2WO_6/Ta_3N_5$ Z-scheme heterojunction nanofibers for efficient degradation of harmful pharmaceutical pollutants. *Chem. Eng. J.*, **2020**, *402*, p.126165.